

PAPER • OPEN ACCESS

## Multipass-friction Stir Processing (MFSP) of Ti-6Al-4V Alloy and Investigation of Flow Properties

To cite this article: Sandip Chougule *et al* 2018 *IOP Conf. Ser.: Mater. Sci. Eng.* **422** 012017

View the [article online](#) for updates and enhancements.



**ECS** **240th ECS Meeting**  
Oct 10-14, 2021, Orlando, Florida

**Register early and save  
up to 20% on registration costs**

Early registration deadline Sep 13

**REGISTER NOW**

# Multipass-friction Stir Processing (MFSP) of Ti-6Al-4V Alloy and Investigation of Flow Properties

Sandip Chougule<sup>1</sup>, Digvijay Sheed<sup>1</sup>, N Prabhu<sup>2</sup>, B P Kashyap<sup>2</sup>, Kaushal Jha<sup>3</sup> and R K P Singh<sup>1</sup>

<sup>1</sup> Bharat Forge, Kalyani Centre for technology and innovation, Pune, 411036, India

<sup>2</sup> Department of Metallurgical Engineering and Materials Science, Indian Institute of Technology Bombay, Mumbai, 400076, India

<sup>3</sup> Engineering design and development division, BARC, Mumbai, 400085, India

E-mail: sandip.chougule@bharatforge.com

**Abstract:** Multipass friction stir processing (MFSP) of the Ti-6Al-4V alloy was carried out at 600 tool rpm and 80 mm/min traverse speed. After first pass, the initial elongated  $\alpha$  structure transformed to prior  $\beta$  grains, consisting of a mixture of acicular  $\alpha'$  and very fine lamellar  $\alpha$  colonies along with  $\alpha$  layer grain boundary in stir zone (SZ). This subsequently transformed to equiaxed  $\alpha$  grain via dynamic recrystallization (DRX) process. With the increase in the number of FSP passes the fraction of equiaxed  $\alpha$  grains was found to increase, reaching almost fully equiaxed  $\alpha$  structure in SZ upon completion of the fifth pass. Flow properties of MFSP Ti-6Al-4V alloy were investigated by differential strain rate test carried out at 927°C. There appears no significant variation in the strain rate sensitivity index ( $m \geq 0.3$ ) values between as received Ti-6Al-4V alloy and MFSP Ti-6Al-4V alloy specimens.

## 1. Introduction

Friction stir processing (FSP) is a solid state processing technique based on the basic principle of friction stir welding (FSW). In recent years, FSP technique is becoming popular along with FSW for many applications, which include producing surface composites, microstructural refinement and homogenization, microstructural modification of metal matrix composites, superplasticity and mechanical property enhancement [1-12]. Up till now, low melting point materials like aluminum alloys, copper alloys and magnesium alloys have been successfully processed via FSW/FSP process [7-9, 13-16], but it faces difficulties with the high melting point materials like titanium alloys, inconel alloys and steel [1]. To overcome these difficulties researchers successfully tried out with different advanced tool materials like tungsten-lanthanum, tungsten-rhenium, tungsten carbides, polycrystalline cubic boron nitride (PCBN) etc. [1,17].

Titanium alloys, especially, the Ti-6Al-4V alloy has been very attractive material for aerospace, bio-medical, marine and petrochemical industries because of its high strength to weight ratio and good corrosion resistance properties [18,19]. Generally, this alloy is joined by using the conventional welding processes like gas tungsten arc welding (GTAW), plasma arc welding, electron beam welding (EBW) etc. However, these processes cause the problems of melting and solidification, large thermal distortion and residual stresses, generated during fusion welding. In order to overcome these problems the friction stir welding technique is found to be a successful one [20]. The success of this technique was reported in Ti-6Al-4V alloy plates ranging from thickness of 1.5 mm to 15 mm of different



starting microstructures [20-31]. The various combinations of tool rotating speed and tool traverse speed were employed in these studies. It was shown that the weld quality or processed surface was mostly affected by tool rotating speed and tool traverse speed. Also, there observed during FSW/FSP are the different process defects like tunnelling voids, flash formation and porosity [2, 14, 16, and 32]. Hence one needs to do experiment with these processing parameters prior to employing the technique for final product. In earlier studies [10-12, 33], significant grain refinement was reported in SZ in the materials undergone FSP. The fine grain size is the most important factor for superplastic behaviour of material which can be achieved by different conventional thermo mechanical processing but it comes with some limitations. In view of the several evidences that FSP can result in grain refinement of bulk materials with an enhanced superplastic behaviour, the Ti-6Al-4V alloy needs to be investigated by friction stir processing and subsequent characterizing for its superplasticity [34, 35].

In present work, MFSP of the Ti-6Al-4V alloy was carried out to study the effect of number of passes on microstructure evolution at each step. Flow properties of as received Ti-6Al-4V alloy and the same upon being subjected to MFSP were evaluated from tensile tests conducted at 927°C by differential strain rate test technique over strain rates  $1 \times 10^{-4} \text{ s}^{-1}$  to  $5 \times 10^{-2} \text{ s}^{-1}$ .

## 2. Material and Experimental work

The material used in this study is mill annealed Ti-6Al-4V alloy in the form of plate of thickness 6 mm. The chemical composition (weight %) is Al 6.29, V 3.96, C 0.007, Fe 0.18, N 0.001, O 0.18 and balance Ti. Considering the low thermal conductivity and high strength of Ti-6Al-4V alloy, the tungsten based tool alloyed with 1 wt. % lanthanum oxide (W-1%L2O3) was used for FSP. The tool design had a shoulder of 25 mm diameter and a tapered pin of length 5.5 mm with the major diameter being 6 mm. In the present work, the tool head was stationary and was tilted at 2° in the traveling direction. Tilt angle of tool was adjusted by indexing the tool head. In MFSP, six passes of FSP were carried out in ambient atmosphere.

After each pass, the specimens were cut along transverse direction of the processed plates for microstructure characterization. Metallographic specimens were prepared on automatic polishing machine Tegramin-30. Etching was done by Kroll's reagent. Microstructure was examined by optical microscopy (OM) and Scanning electron microscopy (SEM). For orientation image microscopy (OIM), the specimens were electro polished in 600 ml methanol, 360 ml ethylene glycol and 60 ml perchloric acid (HClO<sub>4</sub>) solution for 20 seconds at 18 V.

Hardness was measured on the Vickers hardness tester using diamond indenter. To investigate the flow properties by using differential strain rate tests technique [35], sub-size test specimens were machined from MFSP Ti-6Al-4V alloy plates. Differential strain rate tests were performed by using 100 kN capacity, computer controlled servo hydraulic Zwick-Roell Amsler Universal Testing Machine. Tensile specimens were heated to test temperature of 927°C and soaked for 5 minutes in a three in a three zone split furnace before deformation. Then, the test specimens were deformed to total strain of 50% at nine different strain rates varying from  $1 \times 10^{-4} \text{ s}^{-1}$  to  $5 \times 10^{-2} \text{ s}^{-1}$ . Such test was continued on the same samples with the successive strain rate cycling till the failure of test specimens. After deformation, the specimens were water quenched.

## 3. Results and discussion

### 3.1 As-received Ti-6Al-4V microstructure

The as-received Ti-6Al-4V alloy (Mill annealed) used in this study contained elongated  $\alpha$  structure with  $\beta$  phase at the grain boundary as shown in Figure 1.

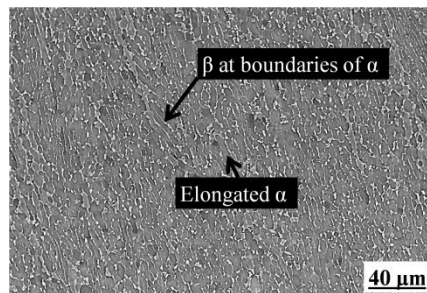
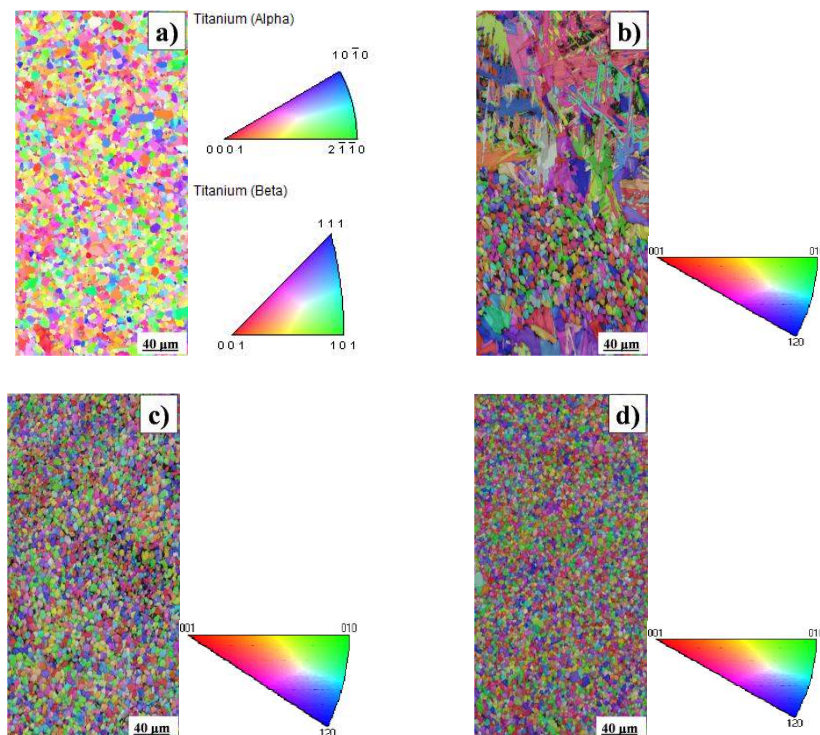


**Figure 1.** SEM image showing microstructure of as-received Ti-6Al-4V alloy

Total fraction of alpha phase ( $\alpha$ ) is 0.927 while that of beta phase ( $\beta$ ) is 0.072. The average grain diameter is 4  $\mu\text{m}$  observed for as-received Ti-6Al-4V alloy.

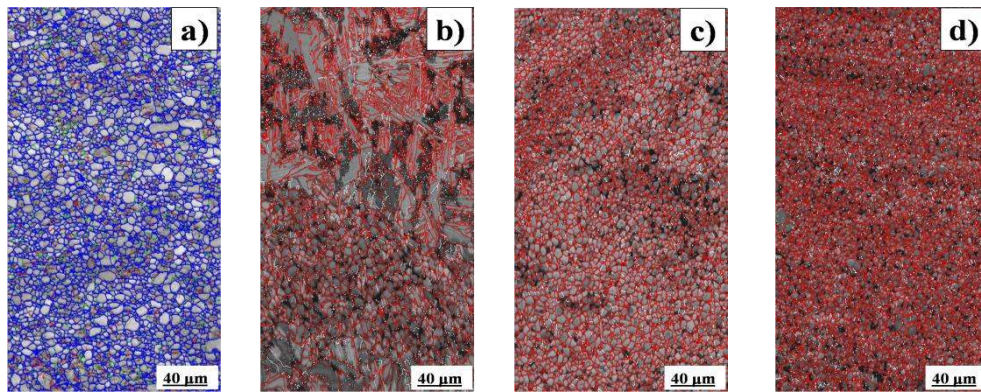
### 3.2 Microstructure evolution:

OIM micrograph in Figure 2 clearly reveals that as received Ti-6Al-4V microstructure consists of  $\alpha$  phase and  $\beta$  phase with random grain orientation. Very less amount of recrystallized  $\beta$  grain fraction is observed in first pass stir zone (SZ) but, upon increasing the number of passes, the fraction of recrystallization is also noted to increase. Finally upon fifth pass, almost whole SZ showed the recrystallized  $\alpha$  grains. After MFSP also, random grain orientation is observed in all the passes. With the increase in strain with increasing FSP pass most of  $\alpha$  grain boundaries become high angle boundaries, which can be clearly observed by red color identification in grain boundary mapping image in Figure 3. This clearly reveals that dynamic recrystallization occurred in  $\beta$  phase region of the multipass friction stir processed specimen. In previous studies, it was found that, in Ti-6Al-4V alloy during deformation in  $\alpha$ - $\beta$  regime, some low angle  $\alpha$  grain boundaries in  $\alpha$  plate existed. This indicates the occurrence of dynamic recovery during deformation. Some dynamically recrystallized  $\alpha$  grains of high angle grain boundaries were also reported by Furuhashi et al. [36].



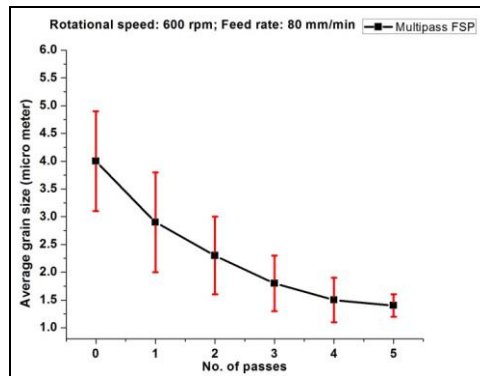
**Figure 2.** Multipass friction stir processed micrographs along with the inverse pole figure (a) As received Ti-6Al-4V alloy (b) First pass, (c) Third pass and (d) Fifth pass.





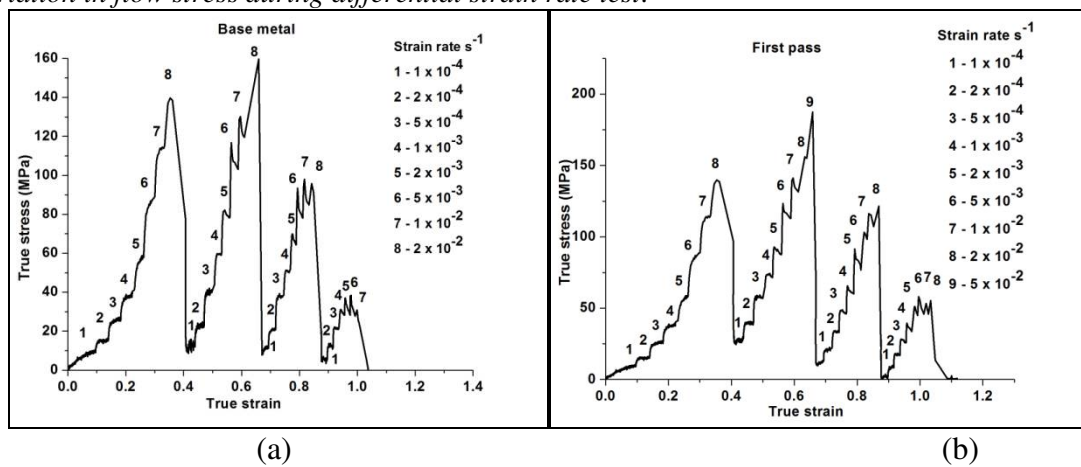
**Figure 3.** High angle grain boundary map of (a) As received Ti-6Al-4V alloy (b) First pass, (c) Third pass and (d) Fifth pass. (Blue color represents low angle grain boundaries whereas red color represents high angle grain boundaries)

Figure 4 shows the variation in average grain size as a function of number of FSP passes, starting from first to fifth pass. It is well understood from the plot that the grain size of material goes on decreasing with increasing number of passes. For first pass, the average grain diameter is 2.9 μm and it goes down to 1.4 μm for fifth pass. This may be due to dynamic recrystallization (DRX) that was observed from second pass till the fifth pass. The plot also shows spread of grain size distribution by the error bar line given.



**Figure 4.** Average grain size of multipass FSP specimens.

3.3 Variation in flow stress during differential strain rate test:



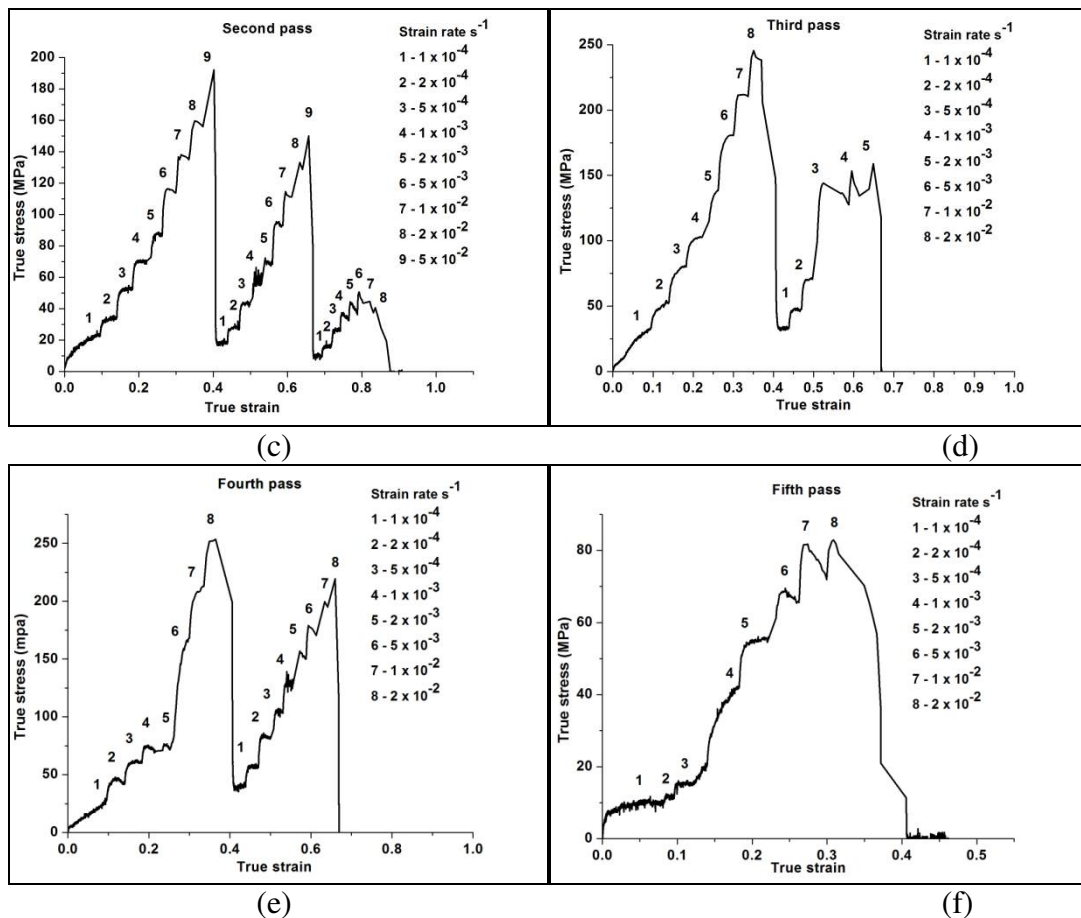


**Figure 5.** True stress vs true strain of (a) As received Ti-6Al-4V (b) First pass FSP (c) Second pass FSP (d) Third pass FSP (e) Fourth pass FSP (f) Fifth pass FSP.

Using the load vs elongation data from differential strain rate test, true stress vs true strain plots are given in the Figure 5 (a-f), for base metal and MFSP specimens. The tests were done from the lowest strain rate of  $1 \times 10^{-4} \text{ s}^{-1}$  to the highest strain rate of  $5 \times 10^{-2} \text{ s}^{-1}$ . On completion of this increasing sequence of strain rate changes, the test was continued but again from the lowest to the highest strain rates. Each series of this sequential increment in strain rate test is termed as a cycle. This way, the samples were deformed as long as they could be without immature necking. The plots are given for a number of strain rate cycling up to the failure of samples. As the number of FSP passes increased, the number of differential strain rate test cycles sustained by specimen was found to reduce. The reason for this could be that as the number of passes increases there occurs an increase in porosity as well as increase in the crack length, which could lead to failure at lower true stress and smaller strain values. This is evident from the differential strain rate test conducted in the sample taken from the fifth pass. Based on true stress vs true strain plots,  $\ln(\text{flow stress})$  vs  $\ln(\text{strain rate})$  were plotted for base metal and MFSP specimens as shown in Figure 6. Superplasticity index, identified by strain rate sensitivity index-  $m \geq 0.3$ , was calculated from the  $\ln(\text{flow stress})$  vs  $\ln(\text{strain rate})$  plot for base metal and MFSP specimens. For as received Ti-6Al-4V alloy and first pass friction stir processed specimens, 'm' values are found to be almost same ( $m = 0.5$ ). As the number of passes increases the flow stress required for deformation increased significantly up to third pass. A decrease in the flow stress is observed for fourth and fifth passes. The 'm' value for second and third passes reduced up to 0.43 at lower strain rates and up to 0.2 at higher strain rates. For the fifth pass, the higher m value of 0.66 is obtained at lower strain rate. Overall, there is successive increase and decrease in the flow stress for MFSP specimens. This successively changing behavior of Ti-6Al-4V alloy MFSP specimens may be due to grain growth or dislocation strengthening of material in second and third passes. The continued deformation beyond this exhibited flow softening, which could be attributed to the mechanisms like

recrystallization or recovery process, that might have occurred in the fourth and fifth pass specimens. Also, the ‘m’ values were also found to successively decrease and increase during MFSP. This may be because of the differences in  $\alpha$  grain morphology developed during MFSP. Microstructure of as received Ti-6Al-4V alloy shows partial elongated grains and it contains 7 % of  $\beta$  phase fraction. The  $\beta$  phase fraction has significant effect on the strain rate sensitivity ‘m’ in Ti-6Al-4V alloy [37].

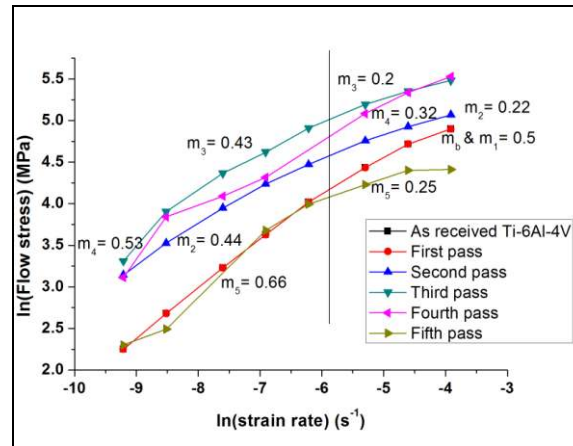


**Figure 6.** ln(flow stress) vs ln(strain rate) of base metal, first pass FSP, second pass FSP, third pass FSP, fourth pass FSP, fifth pass FSP

The grain coarsening of  $\beta$  phase is prevented through partitioning by  $\alpha$  phase. This causes less grain coarsening and so the microstructure remains stable during deformation. In as received Ti-6Al-4V and MFSP samples, at higher strain rate, deformation is almost controlled by dislocation climb mechanism ( $n = 1/m = 4$ ), since  $n$  is stress exponent and is represented as inverse of  $m$  ( $n = 1/m$ ). On the other hand, at lower strain rate, deformation is almost controlled by grain boundary sliding (GBS) mechanism as elaborated in superplastic literature [33]. The fine grain size ( $<10\mu\text{m}$ ) is the most important factor for superplastic behavior of material. Superplasticity is not directly dependent on strain rate, however when the strain rate is very low (approximately  $2 \times 10^{-5} \text{ s}^{-1}$ ), prolonged exposure to high temperature causes grain growth and early failure [38].

#### 4. Conclusions

- Microstructure evolution in the first pass revealed that the initial elongated  $\alpha$  structure transformed to prior  $\beta$  grains, consisting of a mixture of acicular  $\alpha'$  and very fine lamellar  $\alpha/\beta$  colonies in stir zone (SZ). This microstructure subsequently transformed to equiaxed  $\alpha$  with increase in the number of passes. In the fifth pass, fully equiaxed  $\alpha$  structure was observed in SZ. In TMAZ, the prior  $\beta$  grains were decorated with  $\alpha$  layer grain boundary, consisting of lamellar  $\alpha/\beta$  colonies in all the passes. Heat affected zone (HAZ) was characterized by mixture of transformed  $\beta$  grain structure and undeformed  $\alpha$  grains. The mechanism of microstructure evolution in SZ during MFSP is identified to be the occurrence of dynamic recrystallization (DRX) in  $\beta$  phase region.
- For as received Ti-6Al-4V alloy and MFSP specimens, strain rate sensitivity ( $m$ ) value was found to be greater than 0.3. There occurred successive increase and decrease in flow stress for MFSP specimens. The strengthening arises from martensitic phase transformation and grain coarsening in second and third FSP passes, whereas, the subsequent softening in the fourth and fifth FSP passes occurs by dynamic recrystallization or recovery process.

#### 5. References

- [1] Mishra Rajiv S. and Z. Y. Ma. 2005 *Materials Science and Engineering: R* 50 1-78.
- [2] Pilchak A. L., M. C. Juhas and J. C. Williams. 2007 *Metallurgical and Materials Transactions A* 38 401-408.

- [3] Pilchak A. L., D.M. Norfleet, M.C. Juhas and J.C. Williams. 2008 *Metallurgical and Materials Transactions A* 39 1519-1524.
- [4] Sharma S. R., Z. Y. Ma and Rajiv S. Mishra. 2004 *Scripta Materialia* 51 237-241.
- [5] Kwon Y. J., N. Saito and I. Shigematsu. 2002 *Journal of Materials Science Letters* 21 1473-1476.
- [6] Ma Z. Y., S. R. Sharma and Rajiv S. Mishra. 2006 *Scripta materialia* 54 1623-1626.
- [7] Johannes L. B. and R. S. Mishra. 2007 *Materials Science and Engineering: A* 464 255-260.
- [8] Rao A. G., V.A. Katkar, G. Gunasekaran, V.P. Deshmukh, N. Prabhu and B.P. Kashyap 2014 *Corrosion Science* 83198-208.
- [9] Feng A. H. and Z. Y. Ma 2007 *Scripta materialia* 56 397-400.
- [10] Charit I. and Rajiv S. Mishra. 2003 *Materials Science and Engineering: A* 359 290-296.
- [11] Ma Z. Y., R.S. Mishra, M.W. Mahoney and R. Grimes. 2003 *Materials Science and Engineering: A* 351 148-153.
- [12] Ma Z. Y., Rajiv S. Mishra and Murray W. Mahoney. 2002 *Acta materialia* 50 4419-4430.
- [13] Liu G., L.E. Murr, C-S. Niou, J.C. McClure and F.R. Vega. 1997 *Scripta materialia* 37 355-361.
- [14] Park Hwa Soon, Takahiro Kimura, Taichi Murakami, Yoshitaka Naganod, Kazuhiro Nakata and Masao Ushio. 2004 *Materials Science and Engineering: A* 371 160-169.
- [15] Su Jian-Qing, T.W. Nelson, T.R. McNelley and R.S. Mishra. 2011 *Materials Science and Engineering: A* 528 5458-5464.
- [16] Lee Won-Bae, Jong-Woong Kim, Yun-Mo Yeon and Seung-Boo Jung. 2003 *Materials Transactions* 44 917-923.
- [17] Rai R., A. De, H. K. D. H. Bhadeshia and T. DebRoy. 2011 *Science and Technology of welding and Joining* 16 325-342.
- [18] Lütjering Gerd and James Case Williams. 2003 *Titanium*. Vol. 2. Berlin: Springer.
- [19] Leyens Christoph and Manfred Peters. 2003 *Titanium and titanium alloys*. Wiley-VCH, Weinheim.
- [20] Su Jianqing, Rajiv S. Mishra, Jiye Wang, Ray Xu and John A. Baumann. 2013 *Materials Science and Engineering: A* 573 67-74.
- [21] Davies P. S., B.P. Wynne, W.M. Rainforth, M.J. Thomas and P.L. Threadgill. 2011 *Metallurgical and Materials Transactions A* 42 2278-2289.
- [22] Edwards P. D. and M. Ramulu. 2009 *Science and Technology of Welding and Joining* 14 476-483.
- [23] Leo Paola and Emanuela Cerri. 2014 *Materials Science Forum*. Vol. 783 574-579
- [24] Zhang Yu, Yutaka S. Sato, Hiroyuki Kokawa, Seung Hwan C. Park and Satoshi Hirano. 2008 *Materials Science and Engineering: A* 485 448-455.
- [25] Liu H. J., L. Zhou and Q. W. Liu. 2010 *Materials & Design* 31 1650-1655.
- [26] Zhou L., H. J. Liu and Q. W. Liu. 2010 *Materials & Design* 31 2631-2636.
- [27] Pilchak A. L., W. Tang, H. Sahiner, A.P. Reynolds and J.C. Williams. 2011 *Metallurgical and Materials Transactions A* 42 745-762.
- [28] Ramirez Antonio J. and Mary C. Juhas. 2003 *Materials Science Forum*. 426 2999-3004.
- [29] Edwards P. and M. Ramulu. 2010 *Journal of Engineering Materials and Technology* 132 031006.
- [30] Edwards P. and M. Ramulu. 2010 *Science and Technology of Welding & Joining* 15 468-472.
- [31] Ma Z. Y. 2008 *Metallurgical and Materials Transactions A* 39 642-658.
- [32] Chen Hua-Bin, Keng Yan, Tao Lin, Shan-Ben Chen, Cheng-Yu Jiang and Yong Zhao. 2006 *Materials Science and Engineering: A* 433 64-69.
- [33] Nieh Tai-Gang, Jeffrey Wadsworth and O. D. Sherby. 2005 Cambridge university press.
- [34] Kashyap B. P., A. Arieli and A. K. Mukherjee. 1985 *Journal of materials science* 20 2661-2686.
- [35] Kashyap B. P. and G. S. Murty. 1983 *Journal of Materials Science* 18 2063-2070
- [36] Furuhashi Tadashi, B. Poorganji, H. Abe and T. Maki. 2007 *Jom* 59 64-67.
- [37] Sieniawski J. and M. Motyka. 2007 *Journal of Achievements in Materials and Manufacturing Engineering* 24 123-130.



[38] Arieli A. and Rosen A. 1977 *Metallurgical transaction A* 8 1591-1596